# Supporting Information

**Mixed-valent linear $Co^{III}_2Co^{II}$ complexes having easy-axis magnetic anisotropy: experimental and theoretical investigation.**

Naushad Ahmed,[a] Pankaj Kalita, ‡ [b] Rizwan Nabi,[c] Thierry Guizouarn,[d] ‡ Fabrice Pointillart,[d]* [d] Xiaoguang Zhang* [c] and Vadapalli Chandrasekhar * [a]

[a] Tata Institute of Fundamental Research Hyderabad, Gopanpally, Hyderabad-500046, Telangana, India

[b] Department of Chemistry, Nowgong Girls' College, Nagaon, Assam-782001, India

[c] Department of Physics, Center for Molecular Magnetic Quantum Materials, and Quantum Theory Project, University of Florida, Gainesville, Florida 32611, USA

[b] Univ Rennes, CNRS, ISCR (Institut des Sciences Chimiques de Rennes) - UMR 6226, 35000 Rennes, France

[¥] Current Address: Department of Chemistry, Texas A&M University, College Station, Texas 77843, United States

‡ Authors contributed equally

**Table S1.** Crystallographic data and refinement parameters of **1R** and **2S**.

| | **1-R** | **1-S** |
|---|---|---|
| Empirical formula | $C_{74}H_{110}Cl_4Co_3N_4O_{15}$ | $C_{73}H_{106}Cl_4Co_3N_4O_{14}$ |
| Formula weight ($gmol^{-1}$) | 1614.24 | 1582.20 |
| Temperature (K) | 296(2) | 100.00(10) |
| Crystal system | Triclinic | Triclinic |
| Space group | *P*1 | *P*1 |
| Unit cell lengths (Å) | a = 13.099(2)<br>b = 13.535(2)<br>c = 13.677(2) | a = 13.0935(2)<br>b = 13.6028(2))<br>c = 13.6458(2) |
| Unit cell angles (°) | α = 64.280(4)<br>β = 64.970(5)<br>γ = 72.665(5) | α = 64.187(2)<br>β = 65.083(2)<br>γ = 72.5950(10) |
| Volume ($Å^3$) | 1959.9(5) | 1964.25(7) |
| Z | 1 | 1 |
| $\rho_{calc}$ ($g/cm^3$) | 1.368 | 1.338 |
| Absorption coefficient, μ ($mm^{-1}$) | 0.828 | 0.824 |
| F(000) | 851.0 | 833.0 |
| Crystal size ($mm^3$) | 0.41 × 0.32 × 0.2 | 0.35 × 0.2 × 0.12 |
| Radiation | Mo Kα (λ = 0.71073) | Mo Kα (λ = 0.71073) |

| | | |
|---|---|---|
| 2θ range for data collection (°) | 3.374 to 57.368 | 5.674 to 57.918 |
| Reflections collected | 59435 | 54187 |
| Index ranges | $-17 \leq h \leq 17$,<br>$-18 \leq k \leq 18$,<br>$-18 \leq l \leq 18$ | $-17 \leq h \leq 17$,<br>$-18 \leq k \leq 18$,<br>$-17 \leq l \leq 18$ |
| Independent reflections | 19683 [$R_{int}$ = 0.0517] | 17917 [$R_{int}$ = 0.0378] |
| Data/Restrain/Parameter | 19683/138/979 | 17917/296/845 |
| Goodness-of-fit on $F^2$ | 1.038 | 1.072 |
| Final R indices [I>2sigma(I)] | $R_1$ = 0.0671,<br>w$R_2$ = 0.1995 | $R_1$ = 0.0345,<br>w$R_2$ = 0.0792 |
| R indices (all data) | $R_1$ = 0.0861,<br>w$R_2$ = 0.2181 | $R_1$ = 0.0403,<br>w$R_2$ = 0.0816 |
| Largest diff. peak/hole (e Å$^{-3}$) | 1.49/-0.72 | 0.39/-0.41 |
| Flack Parameter | 0.059(7) | 0.039(5) |
| CCDC Number | 2302742 | 2302743 |

**Table S2.** Continuous SHAPE analysis of **1-R** and **1-S**.

| **Complex** | **Polyhedron** | | | | |
|---|---|---|---|---|---|
| | **HP-6** | **PPY-6** | **OC-6** | **TPR-6** | **JPPY-6** |
| **1-R_Co1** | 32.037 | 27.212 | **0.303** | 14.583 | 30.838 |
| **1-R_Co2** | 27.202 | 27.220 | **1.006** | 15.007 | 30.026 |
| **1-R_Co3** | 30.675 | 27.677 | **0.311** | 14.765 | 31.140 |
| **1-S_Co1** | 31.932 | 27.285 | **0.296** | 14.587 | 30.834 |
| **1-S_Co2** | 27.016 | 27.023 | **1.030** | 14.884 | 29.849 |
| **1-S_Co3** | 30.962 | 27.529 | **0.276** | 14.724 | 31.051 |

[!]HP-6: Hexagon ($D_{6h}$); PPY-6: Pentagonal pyramid ($C_{5v}$); OC-6: Octahedron ($O_h$); TPR-6: Trigonal prism ($D_{3h}$); JPPY-6: Johnson pentagonal pyramid J2 ($C_{5v}$

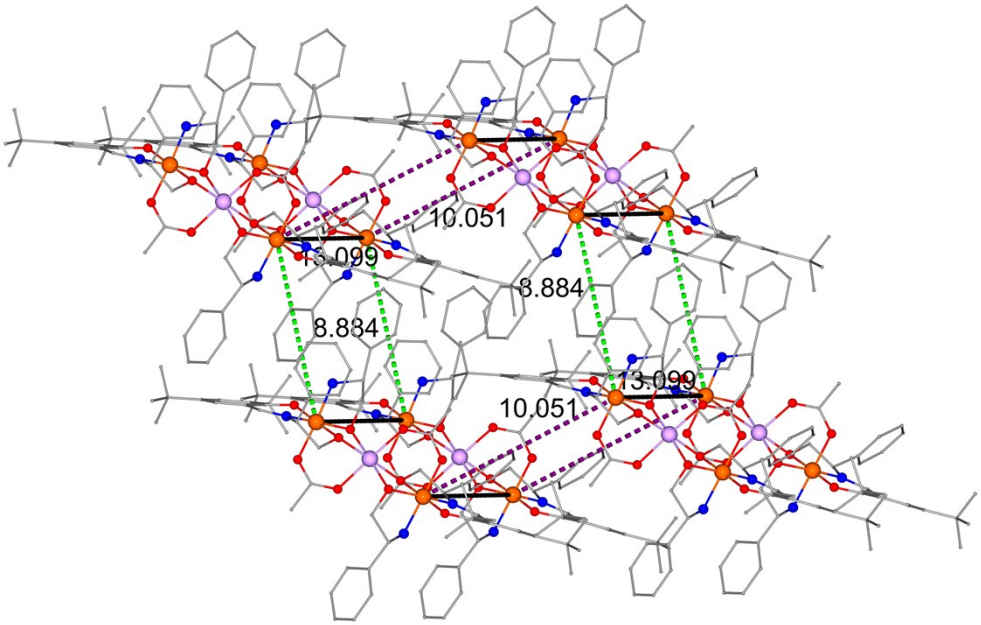


**Figure S1**. Packing structure of **1-R**.

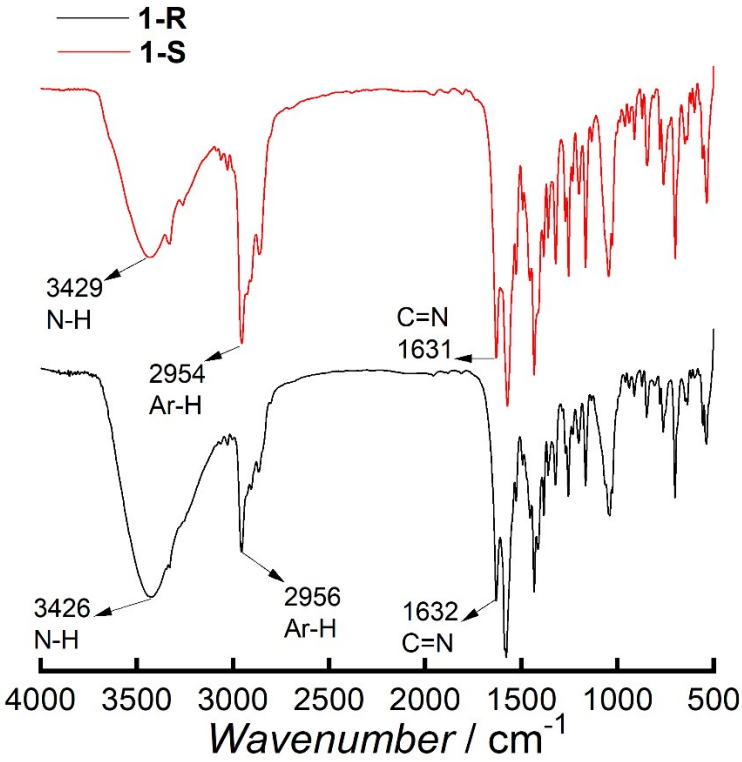


**Figure S2**. FT-IR spectra of **1-R** and **1-S** recorded in KBr matrix.

**BVS Calculations**

The oxidation states of the cobalt metal centres were determined from the metal-ligand bond distances obtained from crystallographic data. Mathematically, the valences of the individual bonds, $s_{ij}$ can be calculated according to equation 1.

$$s_{ij} = exp\left[{(r_0 - r_{ij})}/{b}\right] \qquad \text{.....(Eq. 1)}$$

where i and j represent the donor center and the metal center respectively; $r_0$ is a constant that depends upon the nature of the i–j pair, $r_{ij}$ is the observed bond length, and *b* is usually considered to be 0.37.

According to the BVS postulate, the oxidation state, $z_j$ is the sum of the bond valences of atom j connecting i–j bonds. It is calculated using equation 2.

$$z_j = \sum_i s_{ij} \qquad \text{.....(Eq. 2)}$$

**Table S3**. BVS calculations on **1-R** and **1-S**

| Complex | Atoms | BVS | Assignment |
|---|---|---|---|
| **Complex 1 (1R)** | Co1 | 3.282 | $Co^{3+}$ |
| | Co2 | 2.006 | $Co^{2+}$ |
| | Co3 | 3.229 | $Co^{3+}$ |
| **Complex 2 (2S)** | Co1 | 3.240 | $Co^{3+}$ |
| | Co2 | 1.997 | $Co^{2+}$ |
| | Co3 | 3.243 | $Co^{3+}$ |

**Table S4**. Selected bond length and bond angle parameters for complex **1-R** and **2S**

| **1-R** | | | |
|---|---|---|---|
| **Bond** | **Bond Length (Å)** | **Bond** | **Bond Length (Å)** |
| Co1–O1 | 1.883(8) | Co3–O6 | 1.895(7) |
| Co1–O2 | 1.882(8) | Co3–O7 | 1.891(7) |

| | | | |
|---|---|---|---|
| Co1–O3 | 1.918(7) | Co3–O8 | 1.948(7) |
| Co1–O4 | 1.941(7) | Co3–O9 | 1.918(7) |
| Co1–N1 | 1.879(9) | Co3–N3 | 1.878(8) |
| Co1–N2 | 1.916(9) | Co3–N4 | 1.912(8) |
| Co2–O2 | 2.025(7) | **Bond Angle (°)** | |
| Co2–O3 | 2.132(8) | Co1–Co2–Co3 | 179.16(6) |
| Co2–O5 | 2.106(7) | Co1–O2–Co2 | 98.1(3) |
| Co2–O7 | 2.028(7) | Co1–O3–Co2 | 93.5(3) |
| Co2–O8 | 2.168(7) | Co3–O7–Co2 | 98.7(3) |
| Co2–O10 | 2.105(8) | Co3–O8–Co2 | 92.4(3) |
| **2-S** | | | |
| **Bond** | **Bond Length (Å)** | **Bond** | **Bond Length (Å)** |
| Co1–O1 | 1.882(2) | Co3–O6 | 1.900(2) |
| Co1–O2 | 1.888(2) | Co3–O7 | 1.891(2) |
| Co1–O3 | 1.902(2) | Co3–O8 | 1.949(2) |
| Co1–O4 | 1.935(2) | Co3–O9 | 1.925(2) |
| Co1–N1 | 1.899(3) | Co3–N3 | 1.863(3) |
| Co1–N2 | 1.933(3) | Co3–N4 | 1.923(3) |
| Co2–O2 | 2.040(2) | **Bond Angle (°)** | |
| Co2–O3 | 2.141(2) | Co1–Co2–Co3 | 179.33(2) |
| Co2–O5 | 2.114(2) | Co1–O2–Co2 | 97.68(11) |
| Co2–O7 | 2.031(2) | Co1–O3–Co2 | 93.93(10) |
| Co2–O8 | 2.159(2) | Co3–O7–Co2 | 98.77(10 |
| Co2–O10 | 2.085(2) | Co3–O8–Co2 | 92.77(9) |

**Hirshfeld surface analysis on 1-R**

To understand the major types of intermolecular interactions through short contacts or hydrogen bonding, we have performed Hirshfeld surface analysis on complexes **1-R** and **1-S** using CrystalExplorer 21.5 software.[ref] Several reports on the role of molecules present in secondary coordination sphere revealed that intermolecular interactions can modulate overall dynamic magnetic behaviour of metal complexes.[ref] Both the complexes **1-R** and **1-S** show similar Hirshfeld surface properties and major types of interactions. This is due to their isostructural and enantiomeric relationship. So, we have chosen representative complex **1-R** for our discussion. The computed Hirshfeld surface was mapped in 3D $d_{norm}$ (Fig. 3 a, c and e) which is the summation of $d_i$ and $d_e$ ($d_{norm} = d_{|e|} + d_{|i|}$) where $d_e$ is the closest distance of outside atoms from the surface while $d_i$ is the closest distance of inside atoms from the Hirshfeld surface. 2D finger plots ($d_e$ *vs* $d_i$, Fig. 3 b, d and f) were plotted to show different kind of major interactions present in complex **1-R** (or **1-S**). The major interactions in **1-R** (or **1-S**) were found

through H···H (~70.9%) and H···C ( ~17%) short contacts while interactions through O···H ( ~5%) and Cl···H (~7%) are found to be minor but stronger due to hydrogen bonding. We have compiled the molecular interactions in 3D pi-chart (Fig. 3 g).

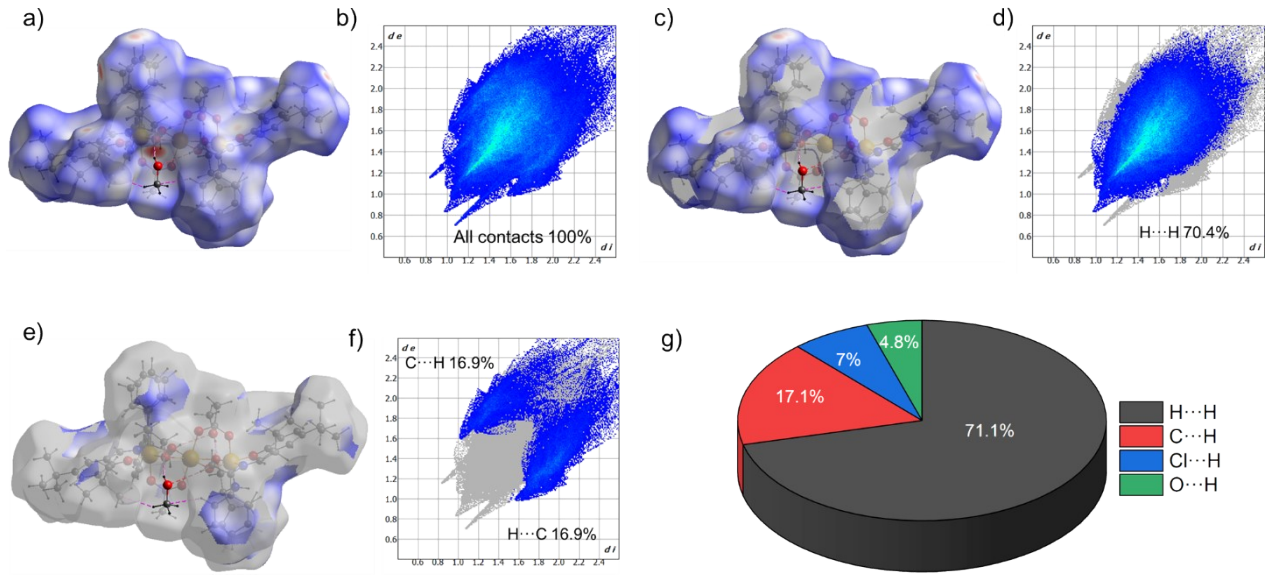


**Figure S3**. Hirshfeld surface mapped in 3D $d_{norm}$ (a, c, and e) interactions for **1-R**. The 2D fingerprint plots (b, d, and f) show the major intermolecular interactions. Yellow dotted lines show the interactions through H-bonding, while magenta dotted lines show short contacts.

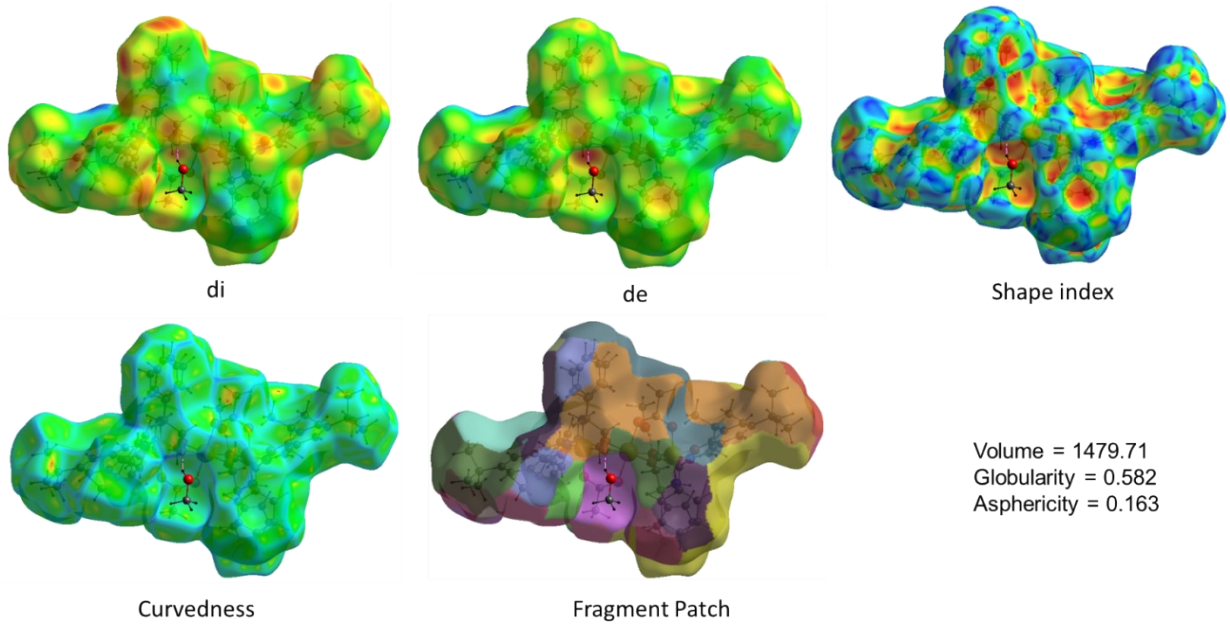


**Figure S4**. Different view of Hirshfeld surface analysis on **1-R**.

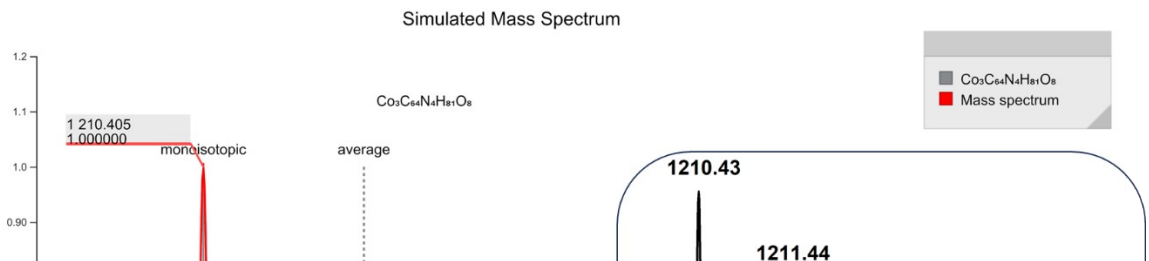

**Figure S5**. Mass data was collected in DCM solvent for **1-R** (inset). The red spectrum shows simulated data corresponding to the molecular formula $Co_3C_{64}N_4H_{81}O_8$, which is associated with the $[Co^{II}Co^{III}_2(R\text{-}L^1)_2(L^2)_2CO_2CH_3]^+$ fragment.

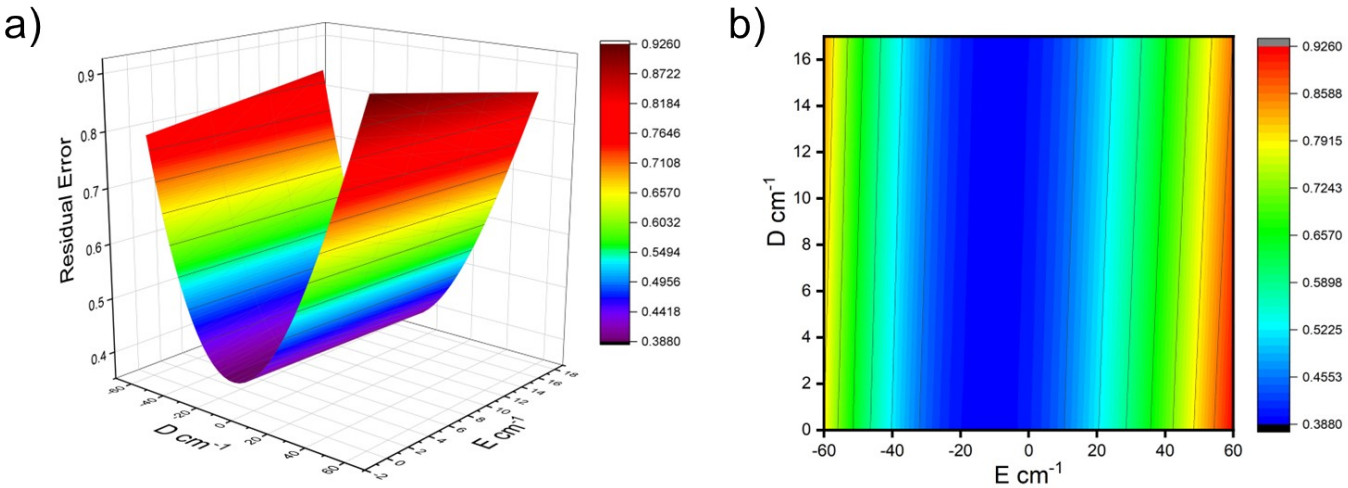


**Figure S6**. 3D survey plots for **1-R**

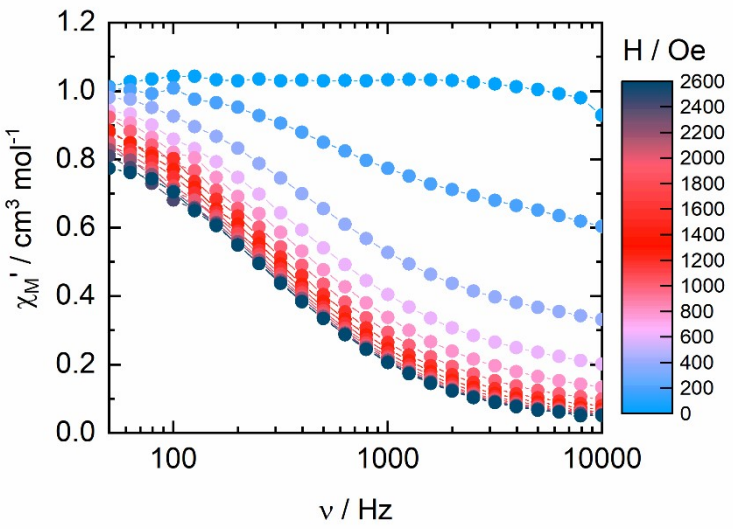


**Figure S7**. Field dependence of the in-phase component of the magnetic susceptibility at 2 K in the field range of 0-2600 Oe for **1-R**.

**The extended Debye model is used for a single relaxation contribution (Eq. S1).**

$$\chi_M' = \chi_S + (\chi_T - \chi_S)\frac{1+(\omega\tau)^{1-\alpha}\sin\left(\alpha\frac{\pi}{2}\right)}{1+2(\omega\tau)^{1-\alpha}\sin\left(\alpha\frac{\pi}{2}\right)+(\omega\tau)^{2-2\alpha}}$$

$$\chi_M'' = (\chi_T - \chi_S)\frac{(\omega\tau)^{1-\alpha}\cos\left(\alpha\frac{\pi}{2}\right)}{1+2(\omega\tau)^{1-\alpha}\sin\left(\alpha\frac{\pi}{2}\right)+(\omega\tau)^{2-2\alpha}}$$

With $\chi_T$ the isothermal susceptibility, $\chi_S$ the adiabatic susceptibility, $\tau$ the relaxation time and $\alpha$ an empiric parameter which describe the distribution of the relaxation time. For SMM with only one relaxing object $\alpha$ is close to zero. The extended Debye model was applied to fit simultaneously the experimental variations of $\chi_M$' and $\chi_M$'' with the frequency $\nu$ of the oscillating field ($\omega = 2\pi\nu$). Typically, only the temperatures for which a maximum on the χ'' vs. *f* curves, have been considered. The best fitted parameters τ, α, $\chi_T$, $\chi_S$ are listed in Tables S5 and S6 with the coefficient of determination $R^2$.

**Table S5**. Best fitted parameters ($\chi_T$, $\chi_S$, $\tau$ and $\alpha$) with the extended Debye model for compound **1-R** at 2 K in the field range 200-2600 Oe.

| H / Oe | $\chi_S$ / cm$^3$ mol$^{-1}$ | $\chi_T$ / cm$^3$ mol$^{-1}$ | α | τ / s | $R^2$ |
|---|---|---|---|---|---|
| 200 | 0.60834 | 1.03747 | 0.23716 | 2.46512E-4 | 0.99954 |
| 400 | 0.3123 | 1.04146 | 0.2414 | 3.49657E-4 | 0.99973 |
| 600 | 0.16535 | 1.06132 | 0.28053 | 4.37223E-4 | 0.99974 |
| 800 | 0.09512 | 1.05803 | 0.2849 | 4.81042E-4 | 0.9996 |
| 1000 | 0.05926 | 1.05308 | 0.28322 | 5.26583E-4 | 0.99963 |
| 1200 | 0.04503 | 1.02409 | 0.2671 | 5.40127E-4 | 0.99933 |
| 1400 | 0.03475 | 1.02305 | 0.2683 | 5.76658E-4 | 0.99958 |
| 1600 | 0.03007 | 0.99439 | 0.26117 | 5.75648E-4 | 0.99965 |
| 1800 | 0.02418 | 0.98825 | 0.26743 | 5.97165E-4 | 0.99965 |
| 2000 | 0.02333 | 0.98034 | 0.26595 | 6.09998E-4 | 0.99893 |
| 2200 | 0.02459 | 0.95502 | 0.25372 | 5.96192E-4 | 0.99948 |
| 2400 | 0.0221 | 0.93088 | 0.255 | 5.84399E-4 | 0.99948 |
| 2600 | 0.0257 | 0.8899 | 0.23146 | 5.35468E-4 | 0.99946 |

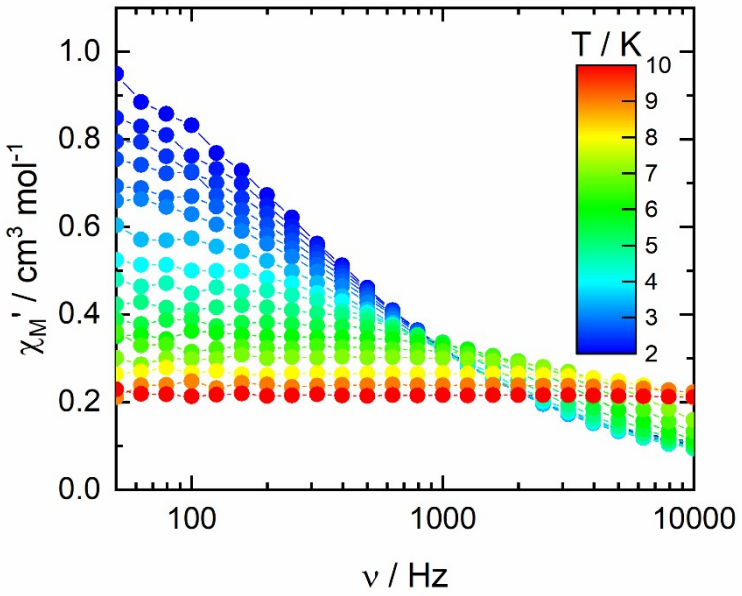


**Figure S8**. Thermal dependence of the in-phase component of the magnetic susceptibility at 1200 Oe in the temperature range of 2-10 K for **1-R**.

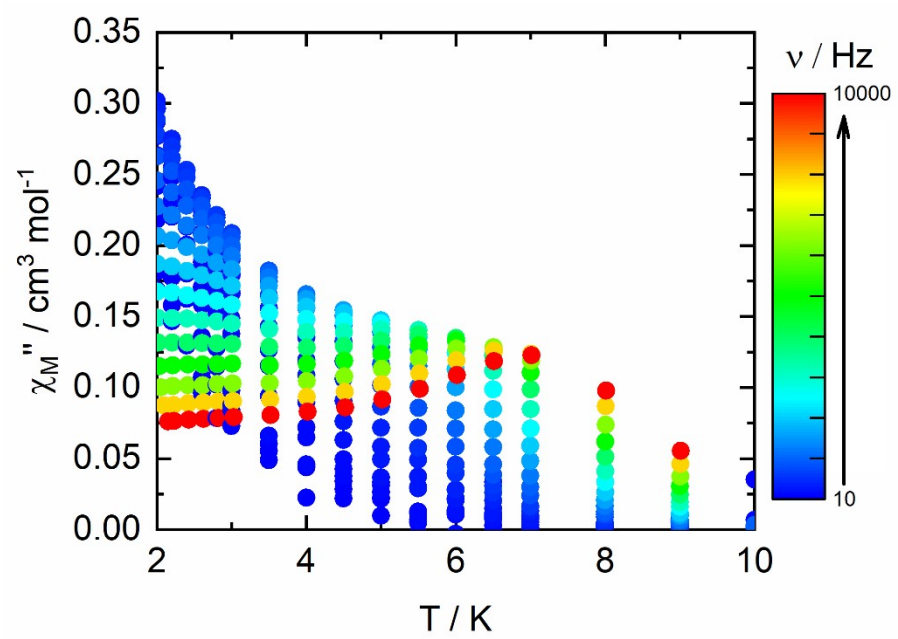


**Figure S9**. Thermal dependence of the out-of-phase component of the magnetic susceptibility under 1.2 kOe applied field from 10 to 10000 Hz frequency range and in the 2-10 K temperature range.

**Table S6**. Best fitted parameters ($\chi_T$, $\chi_S$, $\tau$ and $\alpha$) with the extended Debye model for compound **1-R** at 1200 Oe in the temperature range 2-6 K.

| T / K | $\chi_S$ / cm$^3$ mol$^{-1}$ | $\chi_T$ / cm$^3$ mol$^{-1}$ | α | τ / s | $R^2$ |
|---|---|---|---|---|---|
| 2 | 0.06746 | 1.06029 | 0.29963 | 4.86214E-4 | 0.99892 |
| 2.2 | 0.06 | 0.96826 | 0.30441 | 4.11894E-4 | 0.99961 |
| 2.4 | 0.05608 | 0.8946 | 0.30248 | 3.54562E-4 | 0.99965 |
| 2.6 | 0.05661 | 0.82789 | 0.29098 | 3.06163E-4 | 0.99895 |
| 2.8 | 0.05114 | 0.76067 | 0.28748 | 2.60354E-4 | 0.99948 |
| 3 | 0.04999 | 0.71175 | 0.28038 | 2.31651E-4 | 0.99896 |
| 3.5 | 0.04903 | 0.61837 | 0.26188 | 1.76309E-4 | 0.99842 |
| 4 | 0.05052 | 0.53714 | 0.22778 | 1.30571E-4 | 0.99905 |
| 4.5 | 0.04912 | 0.4816 | 0.20033 | 9.94385E-5 | 0.99879 |
| 5 | 0.05201 | 0.42855 | 0.14804 | 7.22156E-5 | 0.99916 |
| 5.5 | 0.05611 | 0.38608 | 0.09161 | 5.27525E-5 | 0.99875 |
| 6 | 0.05437 | 0.35429 | 0.06057 | 3.78286E-5 | 0.99894 |
| 6.5 | 0.04493 | 0.32989 | 0.06017 | 2.62475E-5 | 0.99714 |

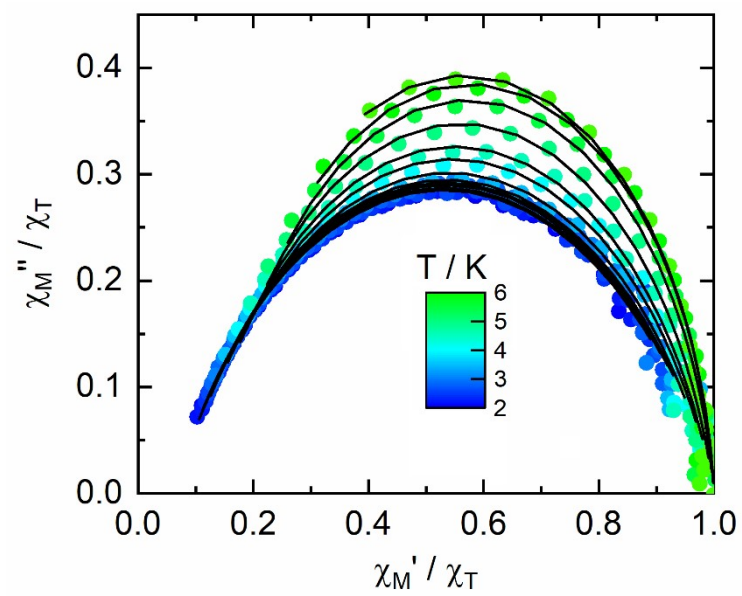


**Figure S10**. Normalized Argand plot for **1-R** at 1200 Oe in the 2-6 K temperature range.

**Table S7**: Hexacoordinate Co(II) complexes reported in the literature and their magnetic parameters

| ***Primary Ligand*** | ***Compound*** | ***D*** | ***E or E/D*** | ***Coordination Environment*** | ***$U_{eff}$*** | ***Ref.*** |
|---|---|---|---|---|---|---|
| ***Mononuclear $Co^{II}$ Complexes#*** | | | | | | |
| 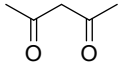 | *$[Co(acac)_2(H_2O)_2]$* | *57/ 63.3* | *-/9.3c* | *O6 Distorted octahedron* | *17 $cm^{-1}$ (300 mT)* | *1* |
| 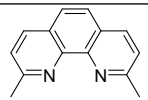 | *$[Co^{II}(dmphen)_2(NCS)_2]$* | *98a/ 146c* | *8.4a/27.0c* | *N6 Highly Distorted octahedron* | *16.2 $cm^{-1}$ (1kG)* | *2* |
| 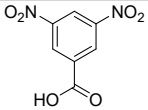 | *$[Co(3,5\text{-}dnb)_2(py)_2(H_2O)_2]$* | *68a/ 117c* | *15a/26.5c* | *N2O4 Octahedron* | *21.1 $cm^{-1}$ (1kOe)* | *3* |
| 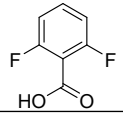 | *$[Co(2,6\text{-}dfba)_2(bpe)_2(H_2O)_2]_n$* | *65.6a/ 122.2c* | *-/4.47c* | *O4N2 Octahedron* | *57.97 K (2kOe)* | *4* |
| 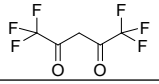 | *$NEt_4[Co(hfac)_3]$* | *+117.8/ +121.2* | *10.04a/ 14.5c* | *N6 Quasi-Octahedral* | *20.6 K (1kOe)* | *5* |
| 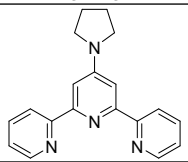 | *$[Co(pyrtpy)_2](BPh_4)_2$* | *-53.6a/ -48.2c* | *5.53a/ 7.37c* | *N6 Highly Distorted octahedron* | *6.8 $cm^{-1}$ (1kOe)* | *6* |
| 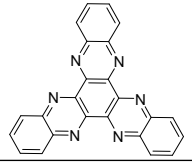 | *$[Co(HATN)(hfca)_2]$* | *-60a* | *-* | *O4N2 Distorted Octahedron* | *17 K (600 Oe)* | *7* |
| 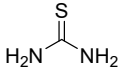 | *$[CoCl_2(L^1)_4]$* | *-63a/ -84c* | *24.7a/18.5c* | *S4Cl2 Octahedron* | *-* | *8* |
| ***Polynuclear $Co^{III}Co^{II}$ Complexes*** | | | | | | |

| | | | | | | |
|---|---|---|---|---|---|---|
| 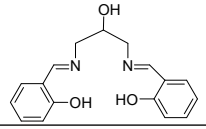 | *$[Co_3(HL)_2(\mu\text{-}AcO)_2(AcO)_2]$* | - | - | *O6*<br>*Distorted octahedron* | - | *9* |
| 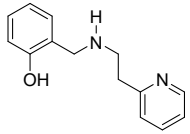 | *$[Co^{III}{}_2Co^{II}(\mu\text{-}OL)_2(\mu\text{-}OOCCH_3)_2(\mu\text{-}N_3)_2(N_3)_2]$* | *±69.5(1) /-83.9 cm1* | *NA/0.244* | *N2O4*<br>*Distorted octahedron* | - | *10* |
| 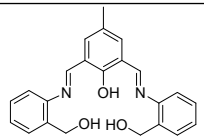 | *$[Co^{III}{}_3Co^{II}(L)(HL)(\mu_4\text{-}O)(\mu\text{-}OH)((CH_3)_3CCOO)_2]$* | *−51.3 cm−1/ −53.6 Cm-1* | | *O5N1*<br>*Distorted Octahedron* | - | *11* |
| 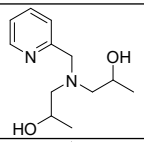 | *$[(pmidip)_2Co_3(CH_3COO)_4]$* | *±36.0 cm–1* | - | *O6*<br>*Distorted octahedral* | - | *12* |
| 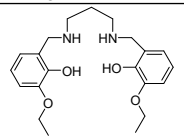 | *$(N_3)Co^{III}L(\mu\text{-}CH_3COO)Co^{II}(N_3)$* | *±5.3 cm-1* | - | *O5N1*<br>*Intermediate between OC & TPR* | | *13* |
| 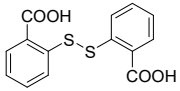 | *$([Co(III)_3Co(II)_2(mba)_6(Hdtba)(H_2O)_4]_n$* | - | - | *O6*<br>*Distorted octahedral and*<br>*O5*<br>*Trigonal bipyramidal geometries* | *34.19 $cm^{-1}$ (1000 Oe)* | *14* |
| 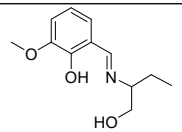 | *$[Co^{II}Co^{III}(L^1)(ab)(mb)_2(H_2O)]$* | *+97.8/+98.1 cm−1,* | *0.008/0.285* | *O6*<br>*Distorted Octahedron* | *12.2 $cm^{-1}$(1000G)* | *15* |
| 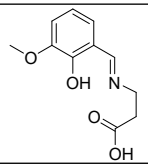 | *$[Co^{III}{}_2Co^{II}(L^2)_4(H_2O)_4]$* | *+55.4cm−1/ 65.8* | *0.000/0.183* | *O6*<br>*Distorted Octahedron* | *10.24 $cm^{-1}$(1000G)* | *15* |
| 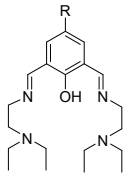 | *$[Co^{III}(N_3)_2L^{Me}(\mu_{1,1}\text{-}N_3)Co^{II}(N_3)]$* | *38.7/42.4* | *0.17* | *N4O1* | - | *16* |

| | | | | | | |
|---|---|---|---|---|---|---|
| | | | | *Distorted Square Pyramidal* | | |
| | *$[Co^{III}(N_3)_2L^{Et}(\mu_{1,1}\text{-}N_3)Co^{II}(N_3)]$* | *NA/45.7* | *0.19* | *N4O1 Distorted Square Pyramidal* | *-* | *16* |
| 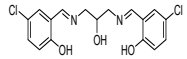 | *$[Co_3(Hclsalpr)_2)(CH_3COO)_4]$* | *-* | *–* | *O6 Distorted Octahedron* | *-* | *17* |
| 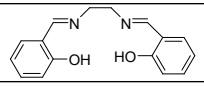 | *$[Co^{II}Co^{III}_2(L)_2(Ph)_2(Cl)_2]$* | *86.9 cm-1/-85.27* | *0.32* | *Cl2O4 Trigonal Prism* | *-* | *18* |
| 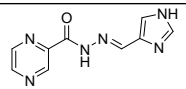 | *$[(L^1)_4Co_3(H_2O)_2](NO_3)_4$* | *35.1* | *-* | *N2O4 Octahedron* | *-* | *19* |
| 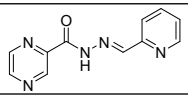 | *$[(L^2)_4Co_3(H_2O)_2](NO_3)_4$* | *48.9* | *-* | *N2O4 Distorted Octahedron* | *5.6 $cm^{-1}$ (1kOe)* | *19* |
| 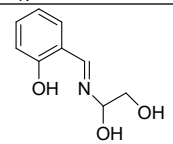 | *$[Co^{III}Co^{II}(HL^1)_2(EtOH)(H_2O)]Cl$* | *±19.9 $cm^{-1}$/+43.8* | *NA/0.184* | *O6 Distorted Octahedral* | *37 K (1kOe) and 7 K (1kOe)* | *20* |
| 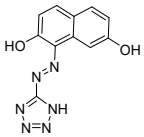 | *$[Co^{II}Co^{III}_2(HATD)_4(H_2O)_4]$* | *-* | *-* | *N2O4 Distorted Octahedron* | *9.12 K and 3.92 K (1000 Oe)* | *21* |
| | *$[Co^{II}Co^{III}_2(HATD)_4(DMF)_2(H_2O)_2]$* | *-* | *-* | *N2O4 Distorted Octahedron* | *8.16 K 1000 Oe* | *21* |
| | *$[Co^{II}_2Co^{III}_2(HATD)_4(bpp)_2(H_2O)_2][Co^{II}(HATD)_2]_2$* | *-* | *-* | *N5O4 Highly Distorted Octahedron* | *24.30 K, 1kOe* | *21* |
| | *$[Co^{II}_2Co^{III}_2(HATD)_4(bpp)_2(H_2O)_2][Co^{III}(HATD)_2]_2$* | *-* | *-* | *N5O4 Highly Distorted Octahedron* | *24.35 K, 1kOe* | *21* |

| | | | | | | |
|---|---|---|---|---|---|---|
| 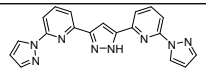 | *$[Co^{II}_2Co^{III}_2LH_4](BF_4)$* | *−82 $cm^{-1}$* | *-* | *N6 Distorted Trigonal Prism* | *16 K (2kOe)* | *22* |
| 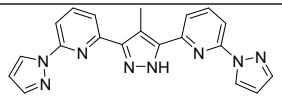 | *$[Co^{II}_2Co^{III}_2LMe_4](BF_4)_6$* | *−78 $cm^{-1}$* | *-* | *N6 Distorted Trigonal Prism* | *26 K, (2kOe)* | *22* |
| 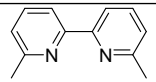 | *$\{[Co^{II}(MeOH)_2][(m\text{-}NC)_2Co^{III}(dmphen)(CN)_2]_2\}_n$* | *+67.0 $cm^{-1}$/+62.7* | *0.13/0.17* | *N4O2 Distorted Octahedron* | *Direct + Raman* | *23* |
| 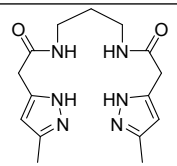 | *$[Co^{II}Co^{III}(L)(DMAP)_3(CH_3COO)]$* | *−25.5* | *2.38* | *N4O2 Irregular five-coordinate geometry* | *49.2 $cm^{-1}$ (1kOe)* | *24* |
| | *$[Co^{II}Co^{III}(L)(4\text{-}Pyrrol)_3(CH_3COO)]$* | *−13.8* | *3.97* | *N4O2 Irregular five-coordinate geometry* | *17.7 $cm^{-1}$ (1kOe)* | *24* |
| 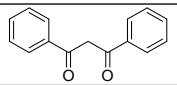 | *$[Co^{II}Co^{III}_2(\mu_3\text{-}OH)(\mu\text{-}pz)_4(DBM)_3]$* | *+23.85* | *~0.17* | *N2O3 Distorted TBP* | *QTM + Raman* | *25* |
| 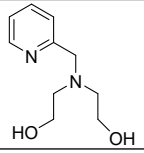 | *$[Co^{III}Co^{II}(pmide)(piv)_3(H_2O)]$ Pivalate* | *±29/±72* | *NA/0.33* | *O6 Distorted Trigonal prism* | *120 $cm^{-1}$, (1.5kOe)* | *26* |
| 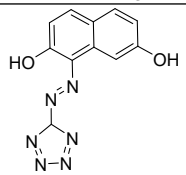 | *$[Co^{II}Co^{III}_2(HATD)_4(H_2O)_4]$* | *+67* | *14.7* | *N4O2 Distorted Octahedral* | *16 $cm^{-1}$ (800 Oe)* | *27* |
| 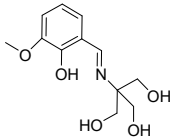 | *$[Co^{III}Co^{II}(LH_2)_2(Cl)(H_2O)]$* | *-7.4* | *< 0.001* | *O5Cl Distorted Octahedron* | *7.9 $cm^{-1}$ (1kOe)* | *28* |
| | *$[Co^{III}Co^{II}(LH_2)_2(Br)(H_2O)]$* | *-9.7* | *< 0.001* | *O5Br Distorted Octahedron* | *14.5 cm-1 (1kOe)* | *28* |
| | *$[Co^{II}Co^{III}(H_2L)_2(CH_3OH)(SCN)]$* | *\|18.7\|* | *E = 0.117* | *O5N* | *NA* | *29* |

| | | | | | | |
|---|---|---|---|---|---|---|
| | | | | *Distorted Octahedron* | | |
| | *$[Co^{II}Co^{III}(LH_2)_2(CH_3COO)(H_2O)]$* | *(145)/ −99.6* | *NA/0.27* | *O6 Distorted Octahedron* | *16.1 K (1kOe)* | *30* |
| 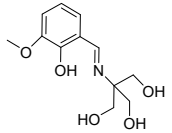 | *$\{[Co_2(H_2L)_2(H_2O)_2][Co_2(H_2L)_2(H_2O)(m\text{-}phth)]$* | *±54.7/–62.4* (cation), –95.8* (anion)* | *NA/0.219, 0.216* | | *16.4 K (500 Oe)* | *31* |
| | *$\{[Co_4(H_2L)_4(H_2O)_2(ppda)]$* | *±60.8/–101.9** | *NA/0.234* | | *22.3 K (500 Oe)* | *31* |
| 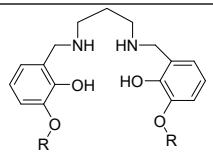 | *$[(NCS)Co^{III}(L^{Me})(\mu\text{–}OAc)Co^{II}(NCS)]$* | | | *O5N Distorted Octahedral geometry* | | *32* |
| | *$[(NCS)Co^{III}(L^{Et})(\mu\text{–}OAc)Co^{II}(NCS)]$* | | | *O5N Distorted Octahedral geometry* | | *32* |
| 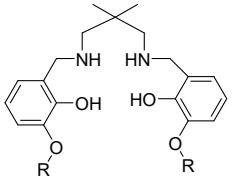 | *$[(NCS)Co^{III}(L^{Me})(\mu\text{–}OAc)Co^{II}(NCS)]$* | | | *O5N Distorted Octahedral geometry* | | *32* |
| | *$[(NCS)Co^{III}(L^{Et})(\mu\text{–}OAc)Co^{II}(NCS)]$* | | | *O5N Distorted Octahedral geometry* | | *32* |
| 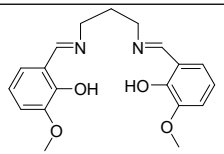 | *$[(N_3)Co^{III}(L^{1r})(\mu\text{-}O_2CR_1)Co^{II}(N_3)][(N_3)Co^{III}(L^{1r})(\mu\text{-}O_2CR_1)Co^{II}Cl]$*<br><br>*$HO_2CR_1$ = 4-nitrobenzoic acid* | – | – | *O5X1 (X = N, Cl) Intermediate between OC & TPR* | *7.3 K (90mT)* | *33* |
| 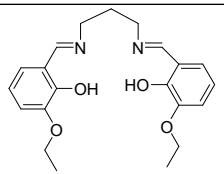 | *$[(N_3)Co^{III}(L^{2r})(\mu\text{-}O_2CR_2)Co_{II}(N_3)][(N_3)Co^{III}(L^{2r})(\mu\text{-}O2CR_2)Co^{II}(OH_2)]ClO_4$*<br><br>*$HO_2CR_2$ = 3-methyl-4-nitrobenzoic acid* | – | – | *O5X1 (X = N, H2O) Intermediate between OC & TPR* | *5.3 K (50mT)* | *33* |

| | | | | | | |
|---|---|---|---|---|---|---|
| 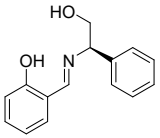 | *[H(NEt$_3$)]$^+$[Co$^{II}$Co$^{III}_3$(L$^{1R}$)$_6$]$^-$* | *−34.4* | *2.54* | *O6 Distorted Trigonal Prism* | *26.6 (0 Oe)* | *34* |
| | *[H(DBU)]$^+$[Co$^{II}$Co$^{III}_3$(L$^{1R}$)$_6$]$^-$* | *−40.6* | *2.13* | *O6 Distorted Trigonal Prism* | *36.4 (0 Oe)* | *34* |
| 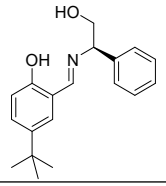 | *[H(NEt$_3$)]$^+$[Co$^{II}$Co$^{III}_3$(L$^{2R}$)$_6$]$^-$* | *−28.8* | *4.88* | *O6 Distorted Trigonal Prism* | *30.0 (0 Oe)* | *34* |
| 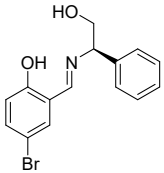 | *[H(DBU)]$^+$[Co$^{II}$Co$^{III}_3$(L$^{3R}$)$_6$]$^-$* | – | – | *O6 Distorted Trigonal Prism* | *88.8 (0 Oe)* | *34* |
| 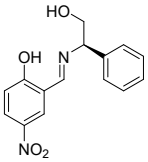 | *[H(DIPEA)]$^+$[Co$^{II}$Co$^{III}_3$(L$^{4R}$)$_6$]$^-$* | – | – | *O6 Distorted Trigonal Prism* | *90.2 (0 Oe)* | *34* |
| | *[H(DBU)]$^+$[Co$^{II}$Co$^{III}_3$(L$^{4R}$)$_6$]$^-$* | – | – | *O6 Distorted Trigonal Prism* | *95.8 (0 Oe)* | *34* |
| | *(n-Bu$_4$N)$^+$[Co$^{II}$Co$^{III}_3$(L$^{4R}$)$_6$]$^-$* | – | – | *O6 Distorted Trigonal Prism* | *102.8 (0 Oe)* | *34* |

Experimental/Theoretical

[#]Representative examples were discussed. For more details on mononuclear $Co^{II}$ complexes, please see the references to 8, 35-37. bpe = 1,2-bis(4-pyridyl)ethylene; py = pyridine, , hfac = exafluoroacetylacetone $H_2$mba = 2-mercaptobenzoic acid; ab = 2-amino-butan-1-ol anion, mb = p-methyl benzoate; bpp = 2,6-di(pyrazol-1-yl)pyridine; DMAP = 4-dimethylaminopyridine; 4-Pyrrol = 4-pyrrolidinopyridine; Pz= pyrazole; piv = Pivalate; phen = 1,10-phenanthroline; m-phth = 1,3-benzenedicarboxylate; ppda = 1,4-phenylenediacrylate; dmf = N,N-dimethylformamide; DBU = 1,8-diazabicyclo[5.4.0]undec-7-ene

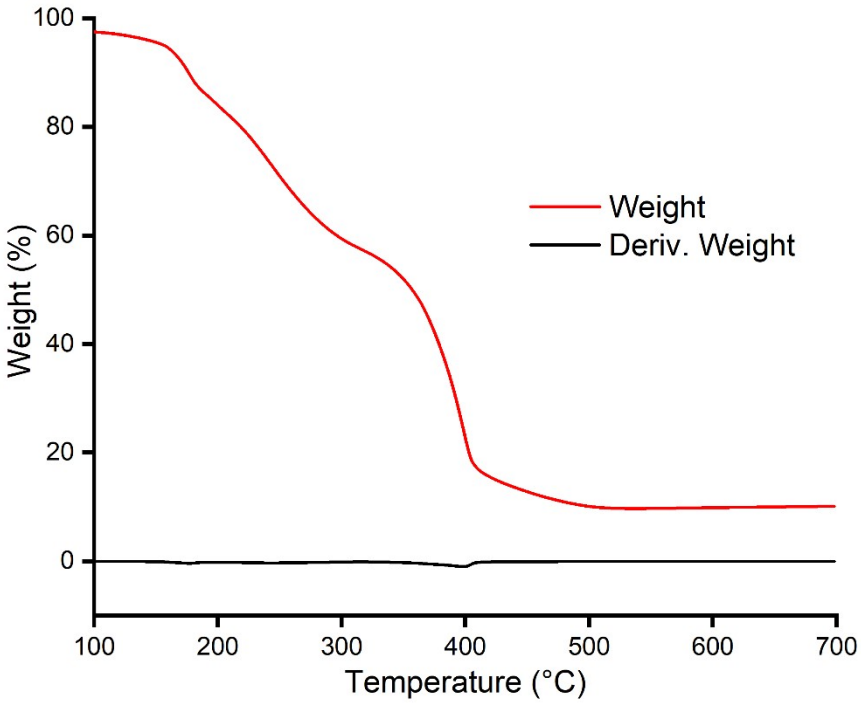


**Figure S11**. Thermogravimetric analysis of complex **1-R**.

**COMPUTATIONAL DETAILS:**

The complete active space self-consistent field (CASSCF) followed by *ab initio* ligand field theory (AILFT) was considered. The NEVPT2 (*n*-electron valence second-order perturbation theory) calculations were also performed on top of the CASSCF wave function to account for the dynamic correlation.[38-40] Here, we employed ZORA in all our calculations. The ZORA type of basis sets, like ZORA-def2-TZVP (triple-$\zeta$ valence polarized) for Co and ZORA-def2-TZVP(-f) for O and ZORA-def2-TZVP for the rest of the atoms, were used during the calculations. While doing the CASSCF-NEVPT2 calculations, we have used 10 quartet roots and 40 doublet roots to calculate the CASSCF and NEVPT2 energies. At the same time, the active space of each Co(II) was comprised of seven electrons in five 3d orbitals of Co(II), CAS(7, 5), which were employed to determine the Zero Field Splitting parameter (ZFS) of the Co(II) ion.

**Table S6**: The ligand field one-electron eigenfunctions of **1-R**.

| Orbital | Energy($cm^{-1}$) | Eigenvalues |
|---|---|---|
| $dx^2$-$y^2$ | 0 | 0.82 |
| dxz | 414.5 | 0.92 |
| dyz | 1188 | 0.89 |
| dxy | 7435 | 0.88 |
| $dz^2$ | 9248.9 | -0.98 |

**Table S7**: Individual contributions to the D-tensor of **1-R**.

| Block | Mult. | Root | *D* | *E* |
|---|---|---|---|---|
| 0 | 4 | 0 | 0 | 0 |
| 0 | 4 | 1 | -75.5 | 0.081 |
| 0 | 4 | 2 | 16.76 | -16.7 |
| 0 | 4 | 3 | 2.623 | 4.521 |
| 0 | 4 | 4 | 1.698 | -0.09 |
| 0 | 4 | 5 | 0.533 | 0.47 |
| 0 | 4 | 6 | 0.013 | -0.01 |
| 0 | 4 | 7 | 0.051 | -0.05 |
| 0 | 4 | 8 | 0.002 | -0.02 |
| 0 | 4 | 9 | -0.07 | 0.001 |
| 1 | 2 | 0 | -3.07 | 1.952 |
| 1 | 2 | 1 | 3.698 | -0.06 |
| 1 | 2 | 2 | 0.153 | 0.056 |
| 1 | 2 | 3 | 0.147 | 0.055 |
| 1 | 2 | 4 | 2.329 | -0.01 |
| 1 | 2 | 5 | -0.27 | 0.331 |
| 1 | 2 | 6 | -0.06 | 0.043 |
| 1 | 2 | 7 | -0.82 | 0.814 |
| 1 | 2 | 8 | -1.52 | -1.53 |
| 1 | 2 | 9 | 0.001 | 0 |
| 1 | 2 | 10 | 0.231 | 0 |
| 1 | 2 | 11 | -0.1 | 0.087 |
| 1 | 2 | 12 | -0.31 | -0.12 |
| 1 | 2 | 13 | -0.07 | 0.036 |
| 1 | 2 | 14 | -0.3 | 0.15 |
| 1 | 2 | 15 | -0.12 | 0.118 |
| 1 | 2 | 16 | 0.286 | 0.055 |
| 1 | 2 | 17 | 0.306 | 0.035 |
| 1 | 2 | 18 | -0.42 | 0.227 |
| 1 | 2 | 19 | 0.769 | -0.02 |
| 1 | 2 | 20 | -0.33 | 0.503 |
| 1 | 2 | 21 | -0.39 | -0.47 |
| 1 | 2 | 22 | 0.209 | -0.07 |
| 1 | 2 | 23 | 0.007 | -0.01 |
| 1 | 2 | 24 | -0.03 | -0.01 |
| 1 | 2 | 25 | -0.04 | -0.01 |
| 1 | 2 | 26 | -0.01 | 0.008 |
| 1 | 2 | 27 | 0.098 | 0.009 |
| 1 | 2 | 28 | -0.07 | 0.064 |

| | | | | |
|---|---|---|---|---|
| 1 | 2 | 29 | -0.14 | -0.14 |
| 1 | 2 | 30 | 0.02 | 0.005 |
| 1 | 2 | 31 | 0.035 | 0.007 |
| 1 | 2 | 32 | 0.167 | -0 |
| 1 | 2 | 33 | -0.02 | 0.024 |
| 1 | 2 | 34 | -0 | 0.001 |
| 1 | 2 | 35 | 0.057 | 0 |
| 1 | 2 | 36 | -0 | 0 |
| 1 | 2 | 37 | -0.01 | 0.005 |
| 1 | 2 | 38 | -0.03 | 0.026 |
| 1 | 2 | 39 | -0.01 | 0.002 |

**Table S8**: NEVPT2 transition energies of **1-R**.

| STATE | ROOT | MULT. | ΔE/cm$^{-1}$ |
|---|---|---|---|
| 0 | 0 | 4 | 0 |
| 0 | 1 | 4 | 852.8 |
| 0 | 2 | 4 | 1604.8 |
| 0 | 3 | 4 | 8440.9 |
| 0 | 4 | 4 | 9005.5 |
| 0 | 5 | 4 | 9297 |
| 0 | 0 | 2 | 10793.1 |
| 0 | 1 | 2 | 12571.1 |
| 0 | 6 | 4 | 17961.5 |
| 0 | 2 | 2 | 18516.3 |
| 0 | 3 | 2 | 18579.8 |
| 0 | 4 | 2 | 19124.5 |
| 1 | 5 | 2 | 19582.3 |
| 1 | 6 | 2 | 19934.9 |
| 1 | 7 | 2 | 20188.9 |
| 1 | 7 | 4 | 21418.4 |
| 1 | 9 | 2 | 22938.8 |
| 1 | 10 | 2 | 22980.8 |
| 1 | 8 | 4 | 23074.1 |
| 1 | 11 | 2 | 23629.5 |
| 1 | 9 | 4 | 24222.5 |
| 1 | 8 | 2 | 25592.6 |
| 1 | 12 | 2 | 27891.3 |
| 1 | 13 | 2 | 28753.9 |
| 1 | 14 | 2 | 28985 |
| 1 | 15 | 2 | 29596.6 |
| 1 | 16 | 2 | 29841.7 |
| 1 | 17 | 2 | 29918.2 |
| 1 | 18 | 2 | 31488.6 |
| 1 | 19 | 2 | 32033 |
| 1 | 21 | 2 | 34067.3 |
| 1 | 20 | 2 | 34069.9 |
| 1 | 22 | 2 | 34972.1 |
| 1 | 23 | 2 | 35486 |
| 1 | 24 | 2 | 35773.7 |
| 1 | 25 | 2 | 36040.1 |
| 2 | 26 | 2 | 36821 |
| 2 | 27 | 2 | 37078.4 |

| | | | |
|---|---|---|---|
| 2 | 28 | 2 | 42739.9 |
| 2 | 29 | 2 | 43008.1 |
| 2 | 30 | 2 | 44232.1 |
| 2 | 31 | 2 | 44275.9 |
| 2 | 32 | 2 | 45355.8 |
| 2 | 33 | 2 | 45776.3 |
| 2 | 34 | 2 | 45924.2 |
| 2 | 35 | 2 | 64517.3 |
| 2 | 36 | 2 | 65154 |
| 2 | 37 | 2 | 66208.1 |
| 2 | 38 | 2 | 67063.4 |
| 2 | 39 | 2 | 67192.6 |

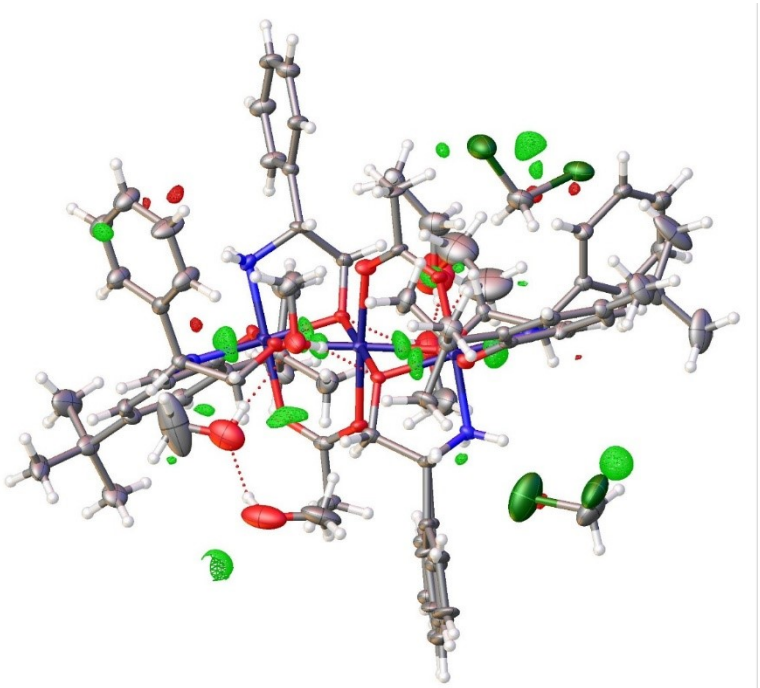

**Figure S12.** Visualizations of the residual density distribution of **1-R**. The residual density was calculated using Olex2 and plotted on a grid of 0.1 Å with an iso-value of 0.70 eÅ$^{-3}$ (green = positive, red = negative).

**Table S9**. Details of the solvent mask for **1-S**

| Sl. No. | Volume/ Formula Unit (Å$^3$) | Electron Count/ Formula Unit | Contents/Formula Unit |
|---|---|---|---|
| 1 | 475 | 133 | 2 $CH_2Cl_2$, 1 EtOH, 1 $CH_3OH$ |

## References


1. S. Gómez-Coca, A. Urtizberea, E. Cremades, P. J. Alonso, A. Camón, E. Ruiz and F. Luis, Origin of slow magnetic relaxation in Kramers ions with non-uniaxial anisotropy, *Nature Communications*, 2014, **5**, 4300.
2. J. Vallejo, I. Castro, R. Ruiz-García, J. Cano, M. Julve, F. Lloret, G. De Munno, W. Wernsdorfer and E. Pardo, Field-Induced Slow Magnetic Relaxation in a Six-Coordinate Mononuclear Cobalt(II) Complex with a Positive Anisotropy, *Journal of the American Chemical Society*, 2012, **134**, 15704-15707.
3. S. Roy, I. Oyarzabal, J. Vallejo, J. Cano, E. Colacio, A. Bauza, A. Frontera, A. M. Kirillov, M. G. B. Drew and S. Das, Two Polymorphic Forms of a Six-Coordinate Mononuclear Cobalt(II) Complex with Easy-Plane Anisotropy: Structural Features, Theoretical Calculations, and Field-Induced Slow Relaxation of the Magnetization, *Inorganic Chemistry*, 2016, **55**, 8502-8513.
4. Y. Wu, D. Tian, J. Ferrando-Soria, J. Cano, L. Yin, Z. Ouyang, Z. Wang, S. Luo, X. Liu and E. Pardo, Modulation of the magnetic anisotropy of octahedral cobalt(ii) single-ion magnets by fine-tuning the axial coordination microenvironment, *Inorganic Chemistry Frontiers*, 2019, **6**, 848-856.
5. A. V. Palii, D. V. Korchagin, E. A. Yureva, A. V. Akimov, E. Y. Misochko, G. V. Shilov, A. D. Talantsev, R. B. Morgunov, S. M. Aldoshin and B. S. Tsukerblat, Single-Ion Magnet Et4N[CoII(hfac)3] with Nonuniaxial Anisotropy: Synthesis, Experimental Characterization, and Theoretical Modeling, *Inorganic Chemistry*, 2016, **55**, 9696-9706.
6. R. F. Higgins, B. N. Livesay, T. J. Ozumerzifon, J. P. Joyce, A. K. Rappé and M. P. Shores, A family of related Co(II) terpyridine compounds exhibiting field induced single-molecule magnet properties, *Polyhedron*, 2018, **143**, 193-200.
7. M. A. Lemes, F. Magnan, B. Gabidullin and J. Brusso, Impact of nuclearity and topology on the single molecule magnet behaviour of hexaazatrinaphtylene-based cobalt complexes, *Dalton Transactions*, 2018, **47**, 4678-4684.
8. S. Tripathi, S. Vaidya, N. Ahmed, E. Andreasen Klahn, H. Cao, L. Spillecke, C. Koo, S. Spachmann, R. Klingeler, G. Rajaraman, J. Overgaard and M. Shanmugam, Structure-property correlation in stabilizing axial magnetic anisotropy in octahedral Co(II) complexes, *Cell Reports Physical Science*, 2021, **2**.
9. E. Baca-Solis, S. Bernès, H. Vazquez-Lima, M.-E. Boulon, R. E. P. Winpenny and Y. Reyes-Ortega, Synthesis, Electronic, Magnetic and Structural Characterization of New Trinuclear Mixed-Valence CoIII-CoII-CoIII Complex, *ChemistrySelect*, 2016, **1**, 6866-6871.
10. Richa, M. Rathnam, A. Kumar, I. Verma, J. Kłak, J. Cano, A. J. Mota, A. Rajput and H. Arora, Discrete unusual mixed-bridged trinuclear CoIII2CoII and pentanuclear NiII coordination complexes supported by a phenolate-based ligand: theoretical and experimental magneto-structural study, *New Journal of Chemistry*, 2021, **45**, 6053-6066.
11. B. Dutta, E. C. Sañudo, R. Herchel and D. Ray, Ancillary Ligand Coordination Directed Modes of Aggregation in Mixed-Valence Tetranuclear Cobalt Complexes: Synthesis, Structure, Field-Induced SIM Behavior, and Theoretical Insights, *Crystal Growth & Design*, 2023, **23**, 2169-2181.
12. J. W. Shin, A. R. Jeong, S. Y. Lee, C. Kim, S. Hayami and K. S. Min, Trinuclear nickel and cobalt complexes containing unsymmetrical tripodal tetradentate ligands: syntheses, structural, magnetic, and catalytic properties, *Dalton Transactions*, 2016, **45**, 14089-14100.

13. A. Banerjee, S. Herrero, Á. Gutiérrez and S. Chattopadhyay, Synthesis, structure and magnetic property of a dinuclear cobalt(II/III) complex with a reduced Schiff base ligand, *Polyhedron*, 2020, **190**, 114756.
14. J. Zhu, B. Liu, W. Zhang, J. Jiang and X. Li, Slow magnetic relaxation in mixed-valence coordination polymer, containing Co(III) cluster and Co(II) nodes, *Journal of Molecular Structure*, 2021, **1230**, 129934.
15. A. Paul, M. Viciano-Chumillas, H. Puschmann, J. Cano and S. C. Manna, Field-induced slow magnetic relaxation in mixed valence di- and tri-nuclear CoII–CoIII complexes, *Dalton Transactions*, 2020, **49**, 9516-9528.
16. S. Mandal, S. Mondal, C. Rajnák, J. Titiš, R. Boča and S. Mohanta, Syntheses, crystal structures and magnetic properties of two mixed-valence Co(iii)Co(ii) compounds derived from Schiff base ligands: field-supported single-ion-magnet behavior with easy-plane anisotropy, *Dalton Transactions*, 2017, **46**, 13135-13144.
17. M. Mikuriya, Y. Naka, A. Inaoka, M. Okayama, D. Yoshioka, H. Sakiyama, M. Handa and M. Tsuboi, Mixed-Valent Trinuclear CoIII-CoII-CoIII Complex with 1,3-Bis(5-chlorosalicylideneamino)-2-propanol.*Journal*, 2022, **27**.
18. S. Hazra, C. Rajnák, J. Titiš, M. F. C. Guedes da Silva, R. Boča and A. J. L. Pombeiro, A Mixed Valence CoIICoIII2 Field-Supported Single Molecule Magnet: Solvent-Dependent Structural Variation.*Journal*, 2021, **26**.
19. D. Wu, X. Zhang, P. Huang, W. Huang, M. Ruan and Z. W. Ouyang, Tuning Transverse Anisotropy in CoIII–CoII–CoIII Mixed-Valence Complex toward Slow Magnetic Relaxation, *Inorganic Chemistry*, 2013, **52**, 10976-10982.
20. R. Modak, B. Mondal, Y. Sikdar, J. Banerjee, E. Colacio, I. Oyarzabal, J. Cano and S. Goswami, Slow magnetic relaxation and water oxidation activity of dinuclear CoIICoIII and unique triangular CoIICoIICoIII mixed-valence complexes, *Dalton Transactions*, 2020, **49**, 6328-6340.
21. M. Yang, Z.-J. Ouyang, Y.-J. Zhong, J.-W. Cai, X.-H. Li and W. Dong, Field-induced slow magnetic relaxation from linear trinuclear CoIII–CoII–CoIII to grid [2 × 2] tetranuclear mixed-valence cobalt complexes, *Dalton Transactions*, 2020, **49**, 17017-17025.
22. J. Tong, S. Demeshko, M. John, S. Dechert and F. Meyer, Redox-Induced Single-Molecule Magnetism in Mixed-Valent [2 × 2] Co4 Grid Complexes, *Inorganic Chemistry*, 2016, **55**, 4362-4372.
23. M.-G. Alexandru, D. Visinescu, S. Shova, J. Cano, N. Moliner, F. Lloret and M. Julve, A Chain of Vertex-Sharing {CoIII2CoII2}n Squares with Single-Ion Magnet Behavior.*Journal*, 2023, **9**.
24. M. Liu, Y. Yang, R. Jing, S. Zheng, A. Yuan, Z. Wang, S.-C. Luo, X. Liu, H.-H. Cui, Z.-W. Ouyang and L. Chen, Slow magnetic relaxation in dinuclear Co(iii)–Co(ii) complexes containing a five-coordinated Co(ii) centre with easy-axis anisotropy, *Dalton Transactions*, 2022, **51**, 8382-8389.
25. A. Collet, G. A. Craig, M. J. Heras Ojea, L. Bhaskaran, C. Wilson, S. Hill and M. Murrie, Slow magnetic relaxation in a {CoIICoIII2} complex containing a high magnetic anisotropy trigonal bipyramidal CoII centre, *Dalton Transactions*, 2018, **47**, 9237-9240.
26. D. Cabrosi, C. Cruz, V. Paredes-García and P. Alborés, A dinuclear Co(iii)/Co(ii) complex based on the H2pmide ligand showing field-induced SMM behaviour, *Dalton Transactions*, 2023, **52**, 175-184.
27. Y.-L. Huang, Y.-J. Zhong, H.-J. Ye, Y.-H. Li, X.-M. Kuang, Z.-J. Ouyang, W.-B. Chen, M. Yang and W. Dong, Slow magnetic relaxation and spin crossover behavior in two

mixed-valence Co(ii)/Co(iii) complexes, *New Journal of Chemistry*, 2022, **46**, 17720-17725.
28. V. Chandrasekhar, A. Dey, A. J. Mota and E. Colacio, Slow Magnetic Relaxation in Co(III)–Co(II) Mixed-Valence Dinuclear Complexes with a CoIIO5X (X = Cl, Br, NO3) Distorted-Octahedral Coordination Sphere, *Inorganic Chemistry*, 2013, **52**, 4554-4561.
29. W. Zhu, S. Zhang, C. Cui, F. Bi, H. Ke, G. Xie and S. Chen, New dinuclear cobalt (II, III) and tetranuclear manganese (III) complexes assembled by a polydentate Schiff-base ligand: synthesis, structure and magnetic properties, *Inorganic Chemistry Communications*, 2014, **46**, 315-319.
30. E. A. Buvaylo, V. N. Kokozay, O. Y. Vassilyeva, B. W. Skelton, A. Ozarowski, J. Titiš, B. Vranovičová and R. Boča, Field-Assisted Slow Magnetic Relaxation in a Six-Coordinate Co(II)–Co(III) Complex with Large Negative Anisotropy, *Inorganic Chemistry*, 2017, **56**, 6999-7009.
31. S. Manna, A. Bhunia, S. Mistri, J. Vallejo, E. Zangrando, H. Puschmann, J. Cano and S. C. Manna, Single-Ion Magnetic Behavior in CoII–CoIII Mixed-Valence Dinuclear and Pseudodinuclear Complexes, *European Journal of Inorganic Chemistry*, 2017, **2017**, 2585-2594.
32. A. Banerjee, C. J. Gómez García, S. Benmansour, R. M. Gomlia, A. Frontera and S. Chattopadhyay, Field-induced single-molecule magnet behaviour in a series of dinuclear cobalt(III,II) complexes, *Polyhedron*, 2022, **220**, 115802.
33. R. S. Sarkar, C. J. Gómez-García, M. G. B. Drew and S. Chattopadhyay, Slow relaxation of the magnetization in two cobalt(iii)/cobalt(ii) dimers, *New Journal of Chemistry*, 2023, **47**, 16913-16926.
34. Y.-Y. Zhu, Y.-Q. Zhang, T.-T. Yin, C. Gao, B.-W. Wang and S. Gao, A Family of CoIICoIII3 Single-Ion Magnets with Zero-Field Slow Magnetic Relaxation: Fine Tuning of Energy Barrier by Remote Substituent and Counter Cation, *Inorganic Chemistry*, 2015, **54**, 5475-5486.
35. S. Tripathi, A. Dey, M. Shanmugam, R. S. Narayanan and V. Chandrasekhar, in *Organometallic Magnets*, eds. V. Chandrasekhar and F. Pointillart, Springer International Publishing, Cham, 2019, DOI: 10.1007/3418_2018_8, pp. 35-75.
36. A. Dey, S. Tripathi, M. Shanmugam, R. S. Narayanan and V. Chandrasekhar, in *Organometallic Magnets*, eds. V. Chandrasekhar and F. Pointillart, Springer International Publishing, Cham, 2019, DOI: 10.1007/3418_2018_9, pp. 77-100.
37. P. Kumar Sahu, R. Kharel, S. Shome, S. Goswami and S. Konar, Understanding the unceasing evolution of Co(II) based single-ion magnets, *Coordination Chemistry Reviews*, 2023, **475**, 214871.
38. C. Angeli, R. Cimiraglia, S. Evangelisti, T. Leininger and J. P. Malrieu, Introduction of n-electron valence states for multireference perturbation theory, *The Journal of Chemical Physics*, 2001, **114**, 10252-10264.
39. C. Angeli, R. Cimiraglia and J.-P. Malrieu, N-electron valence state perturbation theory: a fast implementation of the strongly contracted variant, *Chemical Physics Letters*, 2001, **350**, 297-305.
40. C. Angeli, R. Cimiraglia and J.-P. Malrieu, n-electron valence state perturbation theory: A spinless formulation and an efficient implementation of the strongly contracted and of the partially contracted variants, *The Journal of Chemical Physics*, 2002, **117**, 9138-9153.